

Gravitational Amplification of Test-Mass Potential in the Self-gravitating Isothermal Gaseous Systems

Yuta Ito

Abstract

The present work analyzes perturbed potentials due to test mass that is added instantaneously at the center of symmetry of the equilibrium isothermal self-gravitating gases. We examine gravitational amplification in the isothermal sheet, cylinder, and sphere, assuming that the systems are highly collisional and reach a new state of thermal equilibrium after perturbation. Under the assumptions, the isothermal sheet and cylinder amplify gravitational fields due to test sheet and line masses by 68 % and 53 % maximally. On the one hand, in the isothermal sphere, gravitational fields due to test point mass are amplified oscillatorily with radius and show a repulsive effect at large radii.

Keywords: Isothermal sphere, Isothermal cylinder, Isothermal sheet, Gravitational amplification, Collisional self-gravitating systems

1. Introduction

Due to the nature of long-range interactions caused by Newtonian pair-wise potentials of particles, self-gravitating systems exhibit exotic statistical aspects, such as negative specific heat, violent relaxation, statistical ensemble inequality, and so on (Dauhois et al., 2002; Campa et al., 2014). One of the most fundamental but little-discussed collective effects is the amplification of gravitational field due to test mass that is added in self-gravitating systems. The potential due to test mass attracts and reconfigures ambient masses, and reconfigured masses can amplify gravitational field due to test mass. This amplification is the counterpart of the Debye-shielding in plasmas, so it was originally called “gravitational polarization” (Miller, 1966; Gilbert, 1970). Gravitational amplification is expected to occur in every self-gravitating system and to be useful to understand the effects of an emerging mass and interactions via amplified gravitational fields. However, the phenomenon was discussed only for collisionless systems, such as galaxies and dark matters, and for weakly collisional systems, such as globular clusters and nuclear star clusters. Those discussions were carried out in mathematically tractable and/or physically limited settings. The understanding of gravitational amplification is far from being considered matured.

In collisionless self-gravitating systems, relaxation time scale is much longer than the dynamical time scale (e.g., Binney and Tremaine, 2011). The dynamics can be generally described by the Vlasov equation in conjunction with the Poisson equation. The simplest physical setting for gravitational amplification is to add point test mass in an infinite homogeneous collisionless self-gravitating system composed of particles obeying the Maxwellian distribution function (DF)

(Marochnik, 1968; Padmanabhan and Vasanthi, 1985). However, this setting necessarily faces the “Jeans swindle” problem which is a controversy method but may be valid on spatial scales of over 100 Mpc with the cosmological principle (Falco et al., 2013). The origin of this problem is that homogeneous self-gravitating systems can not be correctly described by the Vlasov-Poisson system. Indeed, actual self-gravitating systems are naturally finite and inhomogeneous. The first and only rigorous study on an infinite inhomogeneous system is due to (Gilbert, 1970). Gilbert analyzed gravitational amplification for collisionless isochrone. The work showed that the effective mass, the partial sum of reconfigured masses due to a test-mass perturbation, is amplified maximally by a factor of 2.75. The literature related to test mass added in inhomogeneous systems is little found except for a simplified system (Goodman and Binney, 1984).

Gravitational amplification may affect slow relaxation process in weakly collisional systems. The systems reach Virial equilibria on dynamical time scales t_D (~ 0.1 Myr) due to a rapid change in the self-consistent mean-field potential (Spitzer, 1988; Binney and Tremaine, 2011). Actual stellar systems are composed of finite number N of stars against the assumption of the mean-field approximation, $N \rightarrow \infty$. On the order of Nt_D (~ 1 Gyr), stellar motions deviate substantially from the original smooth orbits determined by the mean-field potential and its cumulative change in velocity dispersion becomes compatible with the average speed of stellar motion. This process is considered slow relaxation and properly described by a generalized kinetic equation for star clusters (Gilbert, 1968). It was derived by a small-parameter- $1/N$ expansion of N -body DF in the N -body Liouville equation. The characteristics of gravitational amplification is supposed to appear as a perturbed potential between “dressed particles” in the correlation function of the kinetic equation, like the Yukawa potential in the

Email address: yutaito30@gmail.com (Yuta Ito)

correlation function of the Boleu-Lenard equation for plasmas (e.g., Montgomery and Tidman, 1964). However, because of its mathematical complication (Heyvaerts, 2010; Chavanis, 2012), there is little quantitative and qualitative analysis has been discussed on gravitational amplification. Exceptions are dynamical or wave phenomena in homogeneous stellar systems Weinberg (1993) and self-gravitating discs (Fouvry et al., 2017) rather than a static configuration.

A common problem in analyzing gravitational amplification in collisionless and weakly-collisional systems is that we must know the explicit analytical forms of orbital periods and isolating integrals for orbiting masses. This can be achieved only for limited configurations, such as isochrones, harmonic oscillators, and Keplerian potential. To avoid this problem and still deepen our understanding of gravitational amplification, the present work employs collisional self-gravitating models, specifically the equilibrium isothermal systems.

In collisional self-gravitating systems, direct head-on collisions between molecules are dominant over dynamical effects in the zeroth-order approximation. For example, assume a typical dense molecular cloud of dimension of 0.1 pc and density of 10^8m^{-3} and composed of H_2 molecules of radius of 0.1 nm. The Knudsen number Kn is $\sim 10^{-8}$. A highly collisional ($\text{Kn} \ll 1$) self-gravitating system can reach a hydrostatic and isothermal equilibrium. Such a system is described by the Lane-Emden equation for the isothermal self-gravitating gaseous systems (e.g., Horedt, 2004). The most often used are the isothermal sheet, cylinder, and sphere models. The isothermal sheet has been used to describe the vertical structure of disk galaxies (Mo et al., 2010). The isothermal cylinder can model some filamentary structures, such as filaments in infrared-dark clouds (Johnstone et al., 2003) and baryon-rich cores of intergalactic filaments (Harford and Hamilton, 2011). The isothermal sphere is useful to model the cores of dense molecular clouds and protostars (Gnedin et al., 2016). To the best of our knowledge, gravitational amplification has not been analyzed for these isothermal systems. In the present work, we show that gravitational amplification occurs in all the isothermal sheet, cylinder, and sphere while the isothermal sphere causes a repulsive gravitational effect.

The present paper is planned as follows. Section 2 explains the isothermal gaseous sheet, cylinder, and sphere. Section 3 explains the perturbation method to examine gravitational amplification in the isothermal models. Section 4 shows the numerical results, and Section 5 is Conclusion.

2. Self-gravitating isothermal gaseous models

The present section describes fundamental features of the self-gravitating isothermal sheet, cylinder, and sphere. We first explain a general mathematical derivation of the isothermal models and then each model's feature briefly.

2.1. Derivation of the isothermal gaseous models

The isothermal gaseous models are typically described by a hydrostatic equation and equation of state for the ideal gas that

are coupled with the Poisson equation. To compare the present work with collisionless systems, we start with the Boltzmann equation for DF $F(\mathbf{r}, \mathbf{v})$ for masses m interacting via pair-wise Newtonian potential at phase-space point (\mathbf{r}, \mathbf{v}) (Shu, 1991)

$$\left(\frac{\partial}{\partial t} + \mathbf{v} \cdot \frac{\partial}{\partial \mathbf{r}} - \frac{1}{m} \frac{\partial \Phi}{\partial \mathbf{r}} \cdot \frac{\partial}{\partial \mathbf{v}} \right) F(\mathbf{r}, \mathbf{v}, t) = C_{\text{Bol}}(F, F), \quad (2.1)$$

where $C_{\text{Bol}}(F, F)$ is the Boltzmann collision term and $\Phi(\mathbf{r})$ the self-consistent mean-field potential. If head-on collisions dominate system dynamics, or $\text{Kn} \ll 1$, then

$$C_{\text{Bol}}(F, F) = 0. \quad (2.2)$$

A DF that satisfies equation (2.2) is a local Maxwellian DF described in terms of spatial density $n(\mathbf{r}, t)$, bulk velocity $u(\mathbf{r}, t)$, temperature $T(\mathbf{r}, t)$, and energy $E(\mathbf{r}, \mathbf{v}, t)$ available to mass m .

The standard theory for the isothermal models assumes a hydrostatic equilibrium, which corresponds to that the time-independent collisionless Boltzmann equation is valid;

$$\left(\mathbf{v} \cdot \frac{\partial}{\partial \mathbf{r}} - \frac{1}{m} \frac{\partial \Phi}{\partial \mathbf{r}} \cdot \frac{\partial}{\partial \mathbf{v}} \right) F(\mathbf{r}, \mathbf{v}) = 0. \quad (2.3)$$

We introduce the following local Maxwellian DF F_o that satisfies both the conditions in equations (2.2) and (2.3)

$$F_o(\mathbf{r}, \mathbf{v}) = mn_c \Omega^{D/2} \exp \left[-\frac{E_o(\mathbf{r}, \mathbf{v})}{k_B T} \right], \quad (2.4)$$

$$E_o(\mathbf{r}, \mathbf{v}) \equiv \frac{1}{2} m v^2 + \Phi_o(\mathbf{r}) - \Phi_c, \quad (2.5)$$

$$\Omega \equiv \frac{m}{2\pi k_B T}, \quad (2.6)$$

where n_c is the central number density, T the constant temperature, k_B the Boltzmann constant, $\Phi_o(\mathbf{r})$ the mean-field potential due to DF F_o , and Φ_c the central potential. The exponent D is the dimension of the isothermal models. For example, $D = 1$ for the isothermal sheet, and $D = 2$ for the isothermal cylinder.

From equation (2.4), the Poisson equation for the isothermal gaseous models reads

$$\begin{aligned} \frac{\partial}{\partial \mathbf{r}} \cdot \left(\frac{\partial \Phi_o}{\partial \mathbf{r}} \right) &= 4\pi G \int d^3 \mathbf{v} F_o(\mathbf{r}, \mathbf{v}), \\ &= 4\pi G m n_c \exp \left[-\frac{\Phi_o(\mathbf{r}) - \Phi_c}{k_B T} \right]. \end{aligned} \quad (2.7)$$

Introducing dimensionless variables

$$\phi \equiv \frac{\Phi_o(\mathbf{r}) - \Phi_c}{k_B T}, \quad (2.8)$$

$$\xi \equiv \frac{\mathbf{r}}{L_c} \equiv \left(\frac{4\pi G m n_c}{k_B T} \right)^{1/2} \mathbf{r}, \quad (2.9)$$

The general form of the Lane-Emden equation for the isothermal gases is obtained

$$\frac{\partial}{\partial \xi} \cdot \left(\frac{\partial \phi}{\partial \xi} \right) - \exp[-\phi] = 0. \quad (2.10)$$

To handle different spatial symmetries for the isothermal models, we employ the following modulus of independent variables

$$\xi = |\xi| = \begin{cases} |z|, & \text{(linear symmetry)} \\ \rho, & \text{(cylindrical symmetry)} \\ r, & \text{(spherical symmetry)} \end{cases} \quad (2.11)$$

where $z \in (-\infty, \infty)$, $\rho \in [0, \infty)$, and $r \in [0, \infty)$.

2.2. Isothermal sheet model

The isothermal sheet is a three-dimensional self-gravitating model composed of particles moving everywhere in the configuration spaces but stratified in the z -direction (Spitzer, 1942). The sheet potential ϕ generally depends on the radial component as well on each sheet. The dependence, however, is not essential to discuss perturbation along the z -axis. Hence, we treat the isothermal sheet as a one-dimensional model. Equation (2.10) on one dimension along the z -axis reduces to the isothermal sheet model

$$\frac{d^2\phi}{dz^2} - e^{-\phi} = 0, \quad (2.12)$$

with boundary conditions (BCs)

$$\phi(z=0) = 0, \quad \phi'(z=0) = 0. \quad (2.13)$$

The explicit analytical solution to equation (2.12) is known as

$$\phi(z) = \ln \left[\cosh^2 \left(\frac{z}{\sqrt{2}} \right) \right], \quad (2.14)$$

$$n(z) = e^{-\phi(z)} = \cosh^{-2} \left(\frac{z}{\sqrt{2}} \right). \quad (2.15)$$

The total number of masses is finite (per unit cross section) as follows

$$N = \int_{-\infty}^{\infty} n(z') dz' = 2\sqrt{2}. \quad (2.16)$$

2.3. Isothermal cylinder model

The isothermal cylinder model is also a three-dimensional self-gravitating system and was initially derived as the zeroth-order approximation of gaseous rings (Ostriker, 1964). Consider an infinitely-long cylindrical system aligned with the z -axis and described in terms of radius ρ measured from the z -axis. Then, equation (2.10) reduces to the isothermal cylinder model

$$\frac{d^2\phi}{d\rho^2} + \frac{d\phi}{d\rho} - e^{-\phi} = 0, \quad (2.17)$$

with BCs

$$\phi(\rho=0) = 0, \quad \phi'(\rho=0) = 0. \quad (2.18)$$

The explicit analytical solution to equation (2.17) is known as

$$\phi(\rho) = 2 \ln \left[1 + \frac{\rho^2}{8} \right], \quad (2.19)$$

$$n(\rho) = e^{-\phi(\rho)} = \left(1 + \frac{\rho^2}{8} \right)^{-2}. \quad (2.20)$$

The total number of masses *per cylinder length* is finite as follows

$$N_z = 2\pi \int_0^{\infty} n(\rho) \rho d\rho = 8\pi. \quad (2.21)$$

2.4. Isothermal sphere model

Many aspects of the isothermal sphere were studied in detail by Chandrasekhar (1939). Consider a spherically symmetric system in terms of radius r measured from the center. With this configuration, equation (2.10) reduces to the isothermal sphere model

$$\frac{d^2\phi}{dr^2} + \frac{1}{r} \frac{d\phi}{dr} - e^{-\phi} = 0, \quad (2.22)$$

with BCs

$$\phi(r=0) = 0, \quad \phi'(r=0) = 0. \quad (2.23)$$

The explicit analytical solution to equation (2.22) is not known. Near $r=0$, the solution takes the forms

$$\phi(r \approx 0) = -\frac{r^2}{6} + \frac{1}{120} r^4 + \dots, \quad (2.24)$$

$$\rho(r \approx 0) = 1 - \frac{r^2}{6} + \dots, \quad (2.25)$$

and, as $r \rightarrow \infty$, the asymptotic expressions are

$$\phi(r \rightarrow \infty) \approx \ln \frac{r^2}{2} - \frac{C_1}{r^{1/2}} \cos \left[\frac{\sqrt{7}}{2} \ln r + C_2 \right], \quad (2.26)$$

$$\rho(r \rightarrow \infty) \approx \frac{2}{r^2} \left[1 + \frac{C_1}{r^{1/2}} \cos \left(\frac{\sqrt{7}}{2} \ln r + C_2 \right) \right], \quad (2.27)$$

where C_1 and C_2 are constant. The total number of masses is proportional to radius

$$N = 4\pi \int_0^{\infty} n(r) r^2 dr = 4\pi r^2 \phi'(r \rightarrow \infty) \propto r. \quad (2.28)$$

3. Perturbed potentials due to test mass in the isothermal models

We first describe basic ideas of our perturbation method to examine gravitational amplification for the isothermal models, by extending the mathematical formulation used in Section 2.1. We then derive the Poisson equation for each perturbed isothermal model.

3.1. Perturbation method for the isothermal systems

Imagine that test mass m_p is instantaneously added at the center of the symmetry of one of the isothermal models so that test mass does not break the symmetry of the model. After the perturbation, we may expect the form of DF as follows

$$F(\mathbf{r}, \mathbf{v}) = mn_c \Omega^{D/2} \exp \left[-\frac{E(\mathbf{r}, \mathbf{v})}{k_B T} \right] + \epsilon f_1(\mathbf{r}, \mathbf{v}, t), \quad (3.1)$$

$$E(\mathbf{r}, \mathbf{v}) \equiv E_o(\mathbf{r}, \mathbf{v}) + \epsilon \phi_1(\mathbf{r}, t), \quad (3.2)$$

where ϵ is the perturbation parameter, and $\epsilon \phi_1$ and ϵf_1 are deviations from potential Φ_o and DF $mn_c \Omega^{D/2} \exp[-E(\mathbf{r}, \mathbf{v})/k_B T]$. Then, assume that the system reaches a new thermal equilibrium state. The form of f_1 must be determined so as to satisfy both the high collisionality condition in equation (2.2) and time-independent collisionless Boltzmann equation (2.3). It must be a local Maxwellian DF with constant temperature T . The DF f_1

is described in terms of $E_o(\mathbf{r}, \mathbf{v})$ at the order of ϵ and may have an uncertainty by the factor of a constant A . In equation (3.1), expand functions up to the order of ϵ , then

$$F(\mathbf{r}, \mathbf{v}) = F_o(\mathbf{r}, \mathbf{v}) + \epsilon F_o(\mathbf{r}, \mathbf{v}) \left(A - \frac{1}{k_B T} \phi_1(\mathbf{r}) \right). \quad (3.3)$$

In this equation, the contribution of DF f_1 is only to shift the values of potential ϕ_1 by the constant $A k_B T$. Hence, f_1 is not essential to discuss gravitational fields and may be set to zero;

$$f_1 = 0. \quad (3.4)$$

This treatment for f_1 distinctly differs from that for collisionless systems. Without the collisionality condition in equation (2.2), the general solution to time-independent collisionless Boltzmann equation (2.3) is any function of isolating integrals (Binney and Tremaine, 2011). Gilbert (1970) determined the form of f_1 assuming that test mass gradually appears and that orbital effects are included in an orbit-averaged form of perturbed potential.

Based on the analysis above, we have the Poisson equation perturbed by test mass m_p

$$\frac{\partial}{\partial \mathbf{r}} \cdot \left(\frac{\partial}{\partial \mathbf{r}} [\Phi_o + \epsilon \phi_1] \right) = 4\pi G m n_c \exp \left[-\frac{\Phi_o(\mathbf{r}) - \Phi_c + \epsilon \phi_1}{k_B T} \right] + 4\pi \epsilon G m_p \delta(\mathbf{r}), \quad (3.5)$$

where $\delta(\mathbf{r})$ is the delta function of \mathbf{r} . At the order of ϵ

$$\frac{\partial}{\partial \mathbf{r}} \cdot \left(\frac{\partial \phi_1}{\partial \mathbf{r}} \right) = -\frac{1}{L_c^2} \exp \left[-\frac{\Phi_o(\mathbf{r}) - \Phi_c}{k_B T} \right] \phi_1 + 4\pi G m_p \delta(\mathbf{r}). \quad (3.6)$$

Using the dimensionless variables ξ and ϕ defined in equation (2.9), we obtain a dimensionless form of equation (3.6)

$$\frac{\partial}{\partial \xi} \cdot \left(\frac{\partial \delta \phi}{\partial \xi} \right) + \exp[-\phi] \delta \phi = \delta(\xi), \quad (3.7)$$

where $\delta \phi$ is the dimensionless form of potential ϕ_1 defined as

$$\delta \phi \equiv \frac{\phi_1}{k_B T}, \quad (3.8)$$

and ϵ is defined as

$$\epsilon \equiv \frac{m_p}{m n_c L_c^D}. \quad (3.9)$$

Equation (3.7) must be solved with proper BCs for each isothermal model.

3.2. Perturbed isothermal sheet

Assume that test mass sheet is instantaneously added at $z = 0$ on the xy -plane in the isothermal sheet model, then equation (3.7) reduces to

$$\frac{d^2 \delta \phi}{dz^2} + e^{-\phi} \delta \phi = \delta(z). \quad (3.10)$$

We regularize this equation so it becomes numerically solvable. The *raw* potential due to test sheet mass $\delta(z)$ has a singularity at $z = 0$ as follows

$$\phi_s(z) = \frac{1}{2} |z|, \quad (3.11)$$

where the reference value of potential constant is set to zero. We remove the singularity by defining a regularized DF

$$W(z) \equiv \delta \phi(z) - \frac{1}{2} |z|. \quad (3.12)$$

Then, equation (3.10) reduces to

$$\frac{d^2 W}{dz^2} + e^{-\phi} \left(W + \frac{1}{2} |z| \right) = 0. \quad (3.13)$$

Removing the singularity at $z = 0$ means that gravitational field strengths due to $\delta \phi$ and ϕ_s are canceled out near $z = 0$. Hence, the BC for potential W is at $z = 0$

$$W'(z = 0) = 0. \quad (3.14)$$

Gravitational amplification is expected to only reconfigure a mass distribution, like polarization in plasmas. The effective mass m^* , the partial sum of masses associated with potential $W(z)$, must be zero as $z \rightarrow \infty$. The effective mass is at z

$$\begin{aligned} m^*(z) &= -2 \int_0^z e^{-\phi(z')} \left(W(z') + \frac{1}{2} |z'| \right) dz', \\ &= 2(W'(z) - W'(0)). \end{aligned} \quad (3.15)$$

With the BC (3.14), we hence obtain a BC at $z \rightarrow \infty$

$$W'(z \rightarrow \infty) = 0. \quad (3.16)$$

We numerically solve equation (3.13) with the two BCs (3.14) and (3.16).

3.3. Perturbed isothermal cylinder

We repeat a similar analysis of Section 3.2 for the isothermal cylinder model. Assume that test linear mass aligned with the z -axis is instantaneously added into the isothermal cylinder. The *raw* potential due to the test mass is

$$\phi_s(\rho) = \frac{1}{2\pi} \ln \rho, \quad (3.17)$$

where the reference value of potential constant is set to zero. Define the following regularized DF $W(\rho)$ to remove the singularity of potential $\delta \phi(\rho)$ at $\rho = 0$

$$W(\rho) \equiv \delta \phi(\rho) - \frac{1}{2\pi} \ln \rho. \quad (3.18)$$

With this $W(\rho)$ in the isothermal cylinder, equation (3.7) reduces to

$$\frac{d^2 W}{d\rho^2} + \frac{dW}{d\rho} + e^{-\phi} \left(W + \frac{1}{2\pi} \ln \rho \right) = 0. \quad (3.19)$$

The BC for potential $W(\rho)$ is at $\rho = 0$

$$W'(\rho = 0) = 0. \quad (3.20)$$

With this BC, the effective mass is at radius ρ

$$\begin{aligned} m^*(\rho) &= -2\pi \int_0^\rho e^{-\phi(\rho')} \left(W(\rho') + \frac{1}{2\pi} \ln \rho' \right) d\rho', \\ &= 2\pi \rho W'(\rho). \end{aligned} \quad (3.21)$$

To make $m^*(\rho \rightarrow \infty)$ be zero, we need the following BC at $\rho \rightarrow \infty$

$$W'(\rho \rightarrow \infty) = 0. \quad (3.22)$$

However, $m^*(\rho)$ is proportional to ρ . Potential $W(\rho \rightarrow \infty)$ must asymptotically decay more rapidly than ρ^{-1} . The explicit asymptotic expression is readily obtained, by solving equation (3.19) in the limit of $\rho \rightarrow \infty$, as

$$W'(\rho \rightarrow \infty) = \frac{32}{4\pi\rho^3} (1 + 3 \ln \rho). \quad (3.23)$$

With this equation, $m^*(\rho \rightarrow \infty)$ approaches zero. Hence, equation (3.19) can be solved with the BCs (3.20) and (3.22).

3.4. Perturbed isothermal sphere

Assume that test point mass is instantaneously added at the center of the isothermal sphere. The raw potential due to the mass is

$$\phi_s(r) = -\frac{1}{4\pi r}. \quad (3.24)$$

The following regularized DF is defined to remove the singularity of $\delta\phi(r)$ at $r = 0$

$$W(r) \equiv \delta\phi(r) + \frac{1}{4\pi r}. \quad (3.25)$$

With this $W(r)$ in the isothermal sphere, equation (3.7) reduces to

$$\frac{d^2 W}{dr^2} + \frac{1}{2} \frac{dW}{dr} + e^{-\phi} \left(W - \frac{1}{4\pi r} \right) = 0. \quad (3.26)$$

Because of the divergent factor, $1/4\pi r$, in equation (3.26) at $r = 0$, a BC for a regular potential $W(r)$ must be taken as

$$W'(r = 0) = \frac{1}{8\pi}. \quad (3.27)$$

Using this BC, the effective mass is at radius r

$$\begin{aligned} m^*(r) &= -4\pi \int_0^r e^{-\phi(r')} \left(W(r') - \frac{1}{4\pi r'} \right) dr', \\ &= 4\pi r^2 W'(r). \end{aligned} \quad (3.28)$$

Hence, the following BC at $r \rightarrow \infty$ must be satisfied

$$W'(r \rightarrow \infty) = 0. \quad (3.29)$$

The asymptotic behavior of $W(r)$, however, can not make $m^*(r)$ zero as $r \rightarrow \infty$. Solving equation (3.26) as $r \rightarrow \infty$ provides the following asymptotic expression

$$W(r \rightarrow \infty) = \frac{C_3}{r^{1/2}} \cos \left[\frac{\sqrt{7}}{2} \ln r + C_4 \right], \quad (3.30)$$

where C_3 and C_4 are constant. Accordingly, the effective mass diverges with r , like $\sim \sqrt{r}$. This divergence mathematically originates from the slow decay in the isothermal sphere density at large radii ($n \sim 2/r^2$). It can be easily confirmed, by assuming that $W(r)$ decays in a power-law fashion, that the density

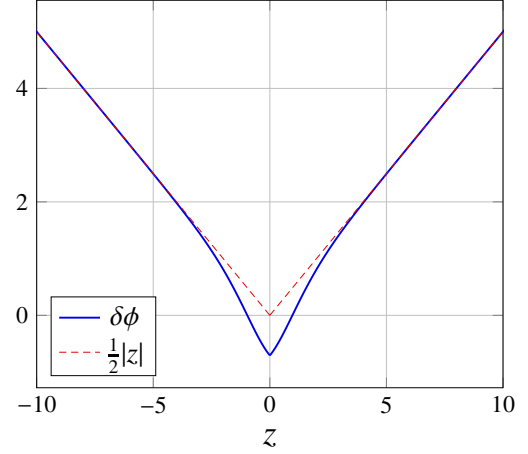


Figure 1: Amplified and raw potentials due to the test mass sheet in the isothermal sheet model.

$n(r)$ must decay more rapidly than r^{-2} to avoid the divergent effective mass. Even though $m^*(r)$ diverges, a physically proper BC at $r \rightarrow \infty$ is still equation (3.29) since it means that gravitational fields due reconfigured mass distribution vanish at large radii. We solve equation (3.26) with the BCs (3.27) and (3.29) after obtaining potential $\phi(r)$ by solving equation (2.22) with the BCs in equation (2.23).

4. Numerical results

The present Section provides the numerical results for the perturbed isothermal models explained in Section 3. We introduce the following quantity as a measure of gravitational amplification

$$\mu = \left| \frac{\delta\phi'(\xi)}{\phi_s'(\xi)} \right|. \quad (4.1)$$

With this measure, if a perturbed gravitational field, $-\delta\phi'$, is amplified then $\mu > 1$ while if it equals the field due to test mass then $\mu = 1$. It turns out that the characteristics of gravitational amplification is quite similar between the isothermal sheet and cylinder. We hence first explain their results, and then the result for the isothermal sphere.

4.1. Numerical results for the isothermal sheet and cylinder

Figures 1 and 2 show perturbed potential $\delta\phi(\xi)$ and unperturbed potential $\phi_s(\xi)$ in the isothermal sheet and cylinder. Figures 3 and 4 depict quantity μ with shifted isothermal sheet- and cylinder- densities. The characteristics of μ is quite similar to the effective mass due to test point mass in the isochrone reported in (Gilbert, 1970). The amplification effect is maximized only once within the system and disappears at $\xi = 0$ and $\xi \rightarrow \infty$. The maximum value of μ is 1.68 at $z \simeq 0.97$ in the isothermal sheet while 1.53 at $\rho \simeq 1.4$ in the isothermal cylinder. The potential $\delta\phi$ behaves like the raw potential ϕ_s at large ξ . This can be easily understood in equations (3.13) and (3.19) in which density dependence becomes weak at large ξ .

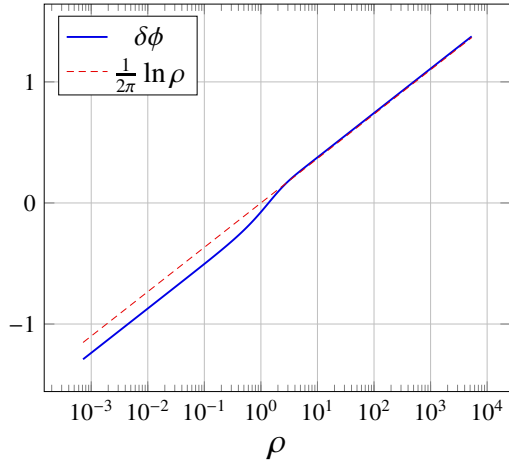


Figure 2: Amplified and raw potentials due to the test mass line in the isothermal cylinder model.

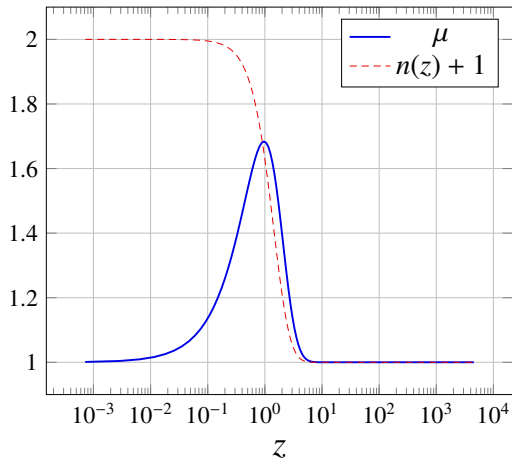


Figure 3: Ratio μ of the amplified potential to the raw potential due to test sheet mass in the isothermal sheet. The density of the isothermal sheet is plotted as a guide for the far-field decay in the ratio.

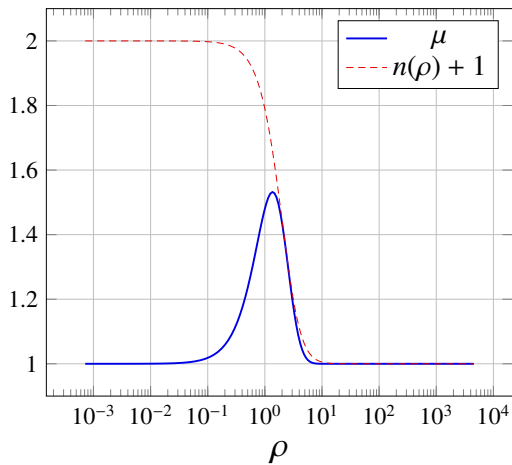


Figure 4: Ratio μ of the amplified potential to the raw potential due to test line mass in the isothermal cylinder. The density of the isothermal cylinder is plotted as a guide for the far-field decay in the ratio.

4.2. Numerical result for the isothermal sphere

Figure 5 shows the potentials $\delta\phi(r)$ and $\phi_s(r)$ in the isothermal sphere. A noteworthy result is that there is a maximum of $\delta\phi(r)$ at $r \simeq 7.7$. Accordingly, the gravitational field vanishes, or is *shielded*. A possibility of gravitational shielding was suggested in an early work (Saslaw, 1968). Saslaw derived a dumped sinusoidal density by using hydrodynamic equations for the isothermal sphere and assuming a growing perturbation like $\sim e^{\sigma t}$ where $\sigma > 0$. Yet, it is not clear whether we should consider Saslaw's and our results as gravitational shielding. Unlike plasma shielding, the perturbed gravitational potentials keep oscillating with radius and do not rapidly converge to a constant value. Figure 6 depicts the quantity μ and a rescaled asymptotic behavior of the effective mass m^* . The quantity μ oscillates with radius, and its amplitude becomes large obeying ($\sim \sqrt{r}$). Hence, the gravitational amplification becomes indefinitely large with radius.

It is noteworthy to point out that particles may feel a repulsive force from test mass at some large radii beyond $r \simeq 7.7$, considering recent interesting observational results (Bialy et al., 2021). They reported shell structures moving toward outward around molecular clouds. The onset of such structures can be readily implied from the structure of perturbed potential $\delta\phi(r)$ in the isothermal sphere. However, the present result is not directly applicable to realistic systems. This is because actual dense clouds are formed in a complicated setting (turbulent multi-component non-spherical open system under the effect of magnetic fields and radiation). More importantly, the isothermal sphere is not stable with infinite radius. It may be stable against radial perturbation due to pressure confinement (Bonnor, 1956). The isothermal sphere in pressure equilibrium with an ambient medium is stable only at radii $r \lesssim 6.5$. Hence, the repulsive effect may not be seen in such a system. On the one hand, if we consider the isothermal sphere confined by an insulated or thermally conductive wall, it can be stable at $r \lesssim 8.99$ or $r \lesssim 34.4$ (D. Lynden-Bell and Royal, 1968). Analyzing gravitational amplification for these toy models appears an interesting topic. It, however, is not directly related to the scope of the present work, so will be discussed in detail somewhere else.

5. Conclusion

The present work examined gravitational amplification in the equilibrium isothermal sheet, cylinder, and sphere. We assumed a high collision limit of head-on particle collisions. Also, we assumed that the isothermal systems reach new isothermal equilibrium states after test-mass perturbation. Hence, the DFs for the systems are a local Maxwellian DF with constant T before and after the perturbation. Test mass is added to each system in a specific way so that the spatial symmetry holds in the system. We used a kinetic formulation to compare the present work to that for collisionless systems.

The numerical results showed that the gravitational amplification in the isothermal sheet and cylinder are quite similar to a known result for collisionless isochrone. The amplification

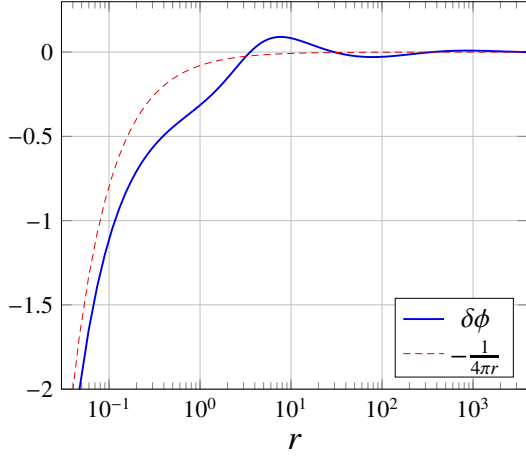


Figure 5: Amplified and raw potentials due to the test point mass in the isothermal sphere.

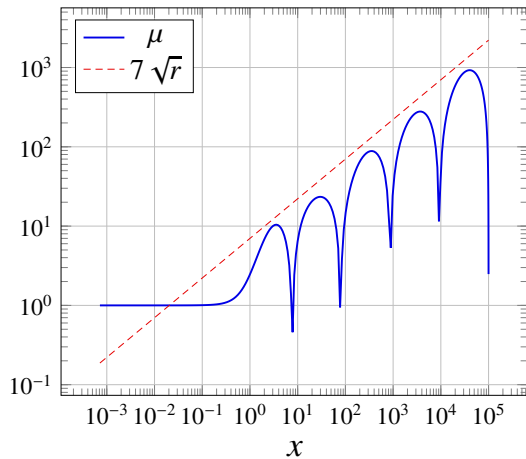


Figure 6: Ratio of the amplified potential to the raw potential due to test point mass in the isothermal sphere. The asymptotic expression of the isothermal sphere is plotted as a guide for the far-field growth in the ratio.

is zero at $r = 0$ and increases with radius until reaching its maximum value. The gravitational field strength is amplified by 68 % maximally in the isothermal sheet while 53 % in the isothermal cylinder. At larger radii, the amplification rapidly diminishes obeying the density decay in the systems.

The isothermal sphere causes an oscillatory gravitational amplification and repulsive effect. However, it is not a consistent result since its effective mass does not reach zero at the infinite radius. Also, the infinite isothermal model is not a stable against radial perturbation. Hence, it is necessary to examine gravitational amplification in a truncated isothermal sphere, avoiding the infinite effective-mass problem and to analyze its stability. With the same reason, analyzing polytropes would be a reasonable extension of the present work. The present paper employed a kinetic formulation to compare the formulation with collisionless systems, but the method is equivalent to the formulation based on hydrostatic equation and the equation of state. So, finite polytropes may be analyzed in a similar fashion.

Since the isothermal cylinder and sheet showed an expected feature of gravitational amplification without facing any mathematical difficulty, we may next take off the assumption used in the present work. For example, we may examine hydrodynamical effects, accordingly time-dependent systems. With this setting, we can examine conditions that test mass perturbation can drive the equilibrium isothermal sheet and cylinder into new equilibrium states. Also, since it is known that these isothermal systems are stable against pressure confinement (Horedt, 1986), we may analyze the stability of the perturbed systems as well. Lastly, examining the effect of more realistic setting on the gravitational amplification is important, such as multi-component, rotational, magnetic-field, and finite-size effects.

Bialy, S., Zucker, C., Goodman, A., Foley, M. M., Alves, J., Semenov, V. A., Benjamin, R., Leike, R., Enßlin, T., sep 2021. The per-tau shell: A giant star-forming spherical shell revealed by 3d dust observations. *The Astrophysical Journal Letters* 919 (1), L5.
URL <https://doi.org/10.3847/2F2041-8213%2Fac1f95>

Binney, J., Tremaine, S., 2011. *Galactic Dynamics*. Princeton university press.
Bonnor, W. B., 1956. Boyle's law and gravitational instability. *Monthly Notices of the Royal Astronomical Society* 116 (3), 351–359.

URL <http://mnras.oxfordjournals.org/content/116/3/351.abstract>
Campa, A., Dauxois, T., Fanelli, D., Ruffo, S., 2014. *Physics of long-range interacting systems*. OUP Oxford.

Chandrasekhar, S., 1939. *An introduction to the study of stellar structure*. Chicago, Ill., The University of Chicago press.

Chavanis, P.-H., jul 2012. Kinetic theory of long-range interacting systems with angle-action variables and collective effects. *Physica A: Statistical Mechanics and its Applications* 391 (14), 3680–3701.
URL <https://doi.org/10.1016%2Fj.physa.2012.02.019>

D. Lynden-Bell, R. W., Royal, A., feb 1968. The gravo-thermal catastrophe in isothermal spheres and the onset of red-giant structure for stellar systems. *Monthly Notices of the Royal Astronomical Society* 138 (4), 495–525.
URL <http://dx.doi.org/10.1093/mnras/138.4.495>

Dauxois, T., Ruffo, S., Arimondo, E., Wilkens, M. (Eds.), 2002. *Dynamics and Thermodynamics of Systems with Long-Range Interactions*. Springer Berlin Heidelberg.
URL <https://doi.org/10.1007%2F3-540-45835-2>

Falco, M., Hansen, S. H., Wojtak, R., Mamon, G. A., jan 2013. Why does the jeans swindle work? *Monthly Notices of the Royal Astronomical Society: Letters* 431 (1), L6–L9.
URL <https://doi.org/10.1093%2Fmnrasl%2Fs1s051>

Fouvy, J.-B., Pichon, C., Chavanis, P.-H., Monk, L., jun 2017. Resonant thickening of self-gravitating discs: imposed or self-induced orbital diffusion in the tightly wound limit. *Monthly Notices of the Royal Astronomical Society*

- 471 (3), 2642–2673.
 URL <https://doi.org/10.1093%2Fmnras%2Fstx1625>
- Gilbert, I. H., jun 1968. Collisional relaxation in stellar systems. *The Astrophysical Journal* 152, 1043.
 URL <https://doi.org/10.1086%2F149616>
- Gilbert, I. H., jan 1970. Gravitational polarization in spherical stellar systems. *The Astrophysical Journal* 159, 239.
- Gnedin, N. Y., Glover, S. C. O., Klessen, R. S., Springel, V., 2016. *Star Formation in Galaxy Evolution: Connecting Numerical Models to Reality*. Springer Berlin Heidelberg.
 URL <http://dx.doi.org/10.1007/978-3-662-47890-5>
- Goodman, J., Binney, J., apr 1984. Adding a point mass to a spherical stellar system. *Monthly Notices of the Royal Astronomical Society* 207 (3), 511–515.
 URL <https://doi.org/10.1093%2Fmnras%2F207.3.511>
- Harford, A. G., Hamilton, A. J., 2011. Intergalactic filaments as isothermal gas cylinders. *Monthly Notices of the Royal Astronomical Society* 416 (4), 2678–2687.
- Heyvaerts, J., jul 2010. A baesescu-lenard-type kinetic equation for the collisional evolution of stable self-gravitating systems. *Monthly Notices of the Royal Astronomical Society* 407 (1), 355–372.
 URL <https://doi.org/10.1111%2Fj.1365-2966.2010.16899.x>
- Horedt, G. P., 1986. Seven-digit tables of Lane-Emden functions. *Astrophysics and Space Science* 126 (2), 357–408.
 URL <http://dx.doi.org/10.1007/bf00639386>
- Horedt, G. P., 2004. *Polytropes*. Kluwer Academic Publishers.
 URL <http://dx.doi.org/10.1007/1-4020-2351-0>
- Johnstone, D., Fiege, J. D., Redman, R., Feldman, P., Carey, S. J., 2003. The g11. 11–0.12 infrared-dark cloud: Anomalous dust and a nonmagnetic isothermal model. *The Astrophysical Journal* 588 (1), L37.
- Marochnik, L. S., 1968. A test star in a stellar system. *Computer Physics Communications* 11, 873.
- Miller, R. H., dec 1966. Polarization of the stellar dynamical medium. *The Astrophysical Journal* 146, 831.
 URL <https://doi.org/10.1086%2F148958>
- Mo, H., Van den Bosch, F., White, S., 2010. *Galaxy formation and evolution*. Cambridge University Press.
- Montgomery, D. C., Tidman, D. A., 1964. *Plasma kinetic theory*. McGraw-Hill Advanced Physics Monograph Series, New York: McGraw-Hill, 1964.
- Ostriker, J., oct 1964. The equilibrium of polytropic and isothermal cylinders. *The Astrophysical Journal* 140, 1056.
 URL <https://doi.org/10.1086%2F148005>
- Padmanabhan, T., Vasanthi, M. M., dec 1985. Gravitational perturbation of homogeneous collisionless dark matter. *Journal of Astrophysics and Astronomy* 6 (4), 247–260.
 URL <https://doi.org/10.1007%2Fbf02715010>
- Saslaw, W. C., jul 1968. Gravithermodynamics – i: Phenomenological equilibrium theory and zero time fluctuations. *Monthly Notices of the Royal Astronomical Society* 141 (1), 1–25.
 URL <https://doi.org/10.1093%2Fmnras%2F141.1.1>
- Shu, F. H., 1991. *The Physics of Astrophysics: Gas Dynamics*. Vol. 2. University Science Books.
- Spitzer, L. J., may 1942. The dynamics of the interstellar medium. III. galactic distribution. *The Astrophysical Journal* 95, 329.
 URL <https://doi.org/10.1086%2F144407>
- Spitzer, L. S., jan 1988. *Dynamical Evolution of Globular Clusters*. Walter de Gruyter GmbH.
 URL <http://dx.doi.org/10.1515/9781400858736>
- Weinberg, M. D., jun 1993. Nonlocal and collective relaxation in stellar systems. *The Astrophysical Journal* 410, 543.
 URL <https://doi.org/10.1086%2F172773>